

Anomalous flux avalanche morphology in a *a*-MoGe superconducting film with a square antidot lattice - experiment and simulation

M. Motta,¹ F. Colauto,¹ W. A. Ortiz,^{1,2} J. I. Vestgården,³ T. H. Johansen,^{2,3,4} Jo Cuppens,⁵ V. V. Moshchalkov,⁵ and A. V. Silhanek⁵

¹*Departamento de Física, Universidade Federal de São Carlos, 13565-905 São Carlos, SP, Brazil*

²*Centre for Advanced Study, Norwegian Academy of Science and Letters, NO-0271, Oslo, Norway*

³*Department of Physics, University of Oslo, POB 1048, Blindern, 0316 Oslo, Norway*

⁴*Institute for Superconducting and Electronic Materials,*

University of Wollongong, Northfields Avenue, Wollongong, NSW 2522, Australia

⁵*INPAC – Institute for Nanoscale Physics and Chemistry, Nanoscale Superconductivity and Magnetism Group, K.U.Leuven, Celestijnenlaan 200D, B-3001 Leuven, Belgium*

(Dated: November 18, 2021)

We have employed magneto-optical imaging to visualize the occurrence of flux avalanches in a superconducting film of *a*-MoGe. The specimen was decorated with square antidots arranged in a square lattice. We observed avalanches with the anomalous habit of forming trees where the trunk is perpendicular to the main axis of the square lattice, whereas the branches form angles of 45 degrees. The overall features of the avalanches, and in particular the 45 degree direction of the branches, were confirmed by numerical simulations.

PACS numbers:

Flux avalanches triggered by thermomagnetic instabilities have been reported in a variety of superconducting films of Nb¹, MgB₂^{2,3}, Nb₃Sn⁴, NbN⁵, YNi₂B₂C⁶, and YBCO⁷. Such events, in which flux bursts suddenly invade the sample, have also been studied in superconducting films decorated with a lattice of antidots, which guide flux motion, as revealed by magneto-optical imaging (MOI) experiments^{9,10}.

The sample investigated in the present work is an amorphous film of MoGe (*a*-MoGe) approximately rectangular in shape, with thickness $t = 25$ nm and lateral dimensions roughly 2.0 mm x 2.6 mm. A square lattice of square antidots (ADs) was fabricated by electron beam lithography. The *a*-MoGe was deposited via pulsed laser deposition from a target of Mo₇₈Ge₂₂ with purity 99.96%, on top of a SiO₂ insulating substrate. The patterned sample has square antidots with sides 0.4 μ m. The period of the pattern is $w = 1.5$ μ m, which corresponds to a commensurability field $H_1 = \frac{\Phi_0}{w^2} = 9.2$ Oe at which the densities of vortices and antidots match each other¹¹. Using the expression for the upper critical field and for the dirty limit¹², the zero temperature superconducting coherence length, $\xi_{GL}(0) = 5$ nm was determined, and the penetration depth, $\lambda_{GL}(0) = 517$ nm was obtained for a similar plain film. Figure 1b shows the orientation of the antidot lattice relative to the edges of the sample.

Characterization measurements of the ac susceptibility and dc magnetization were carried out in commercial Quantum Design equipments (MPMS and PPMS) showing that the superconducting transition temperature at zero field is $T_c = 6.74$ K. The MOI technique employed relies on the Faraday effect¹³ of a garnet indicator film placed on top of the superconducting specimen. The indicator used in the present work was a Bi-substituted yttrium iron garnet film (Bi:YIG) with in-plane magnetization.

Figure 1a shows a magneto optical image taken at $T = 4.5$ K and an applied DC field of $H = 1$ Oe. Noticeably, the main trunk of the tree-like avalanches are predominantly perpendicular to one of the sample edges whereas, surprisingly, the branches form angles of 45 degrees relative to the main axes of the antidot lattice. Avalanches directed at 45 degrees have previously been observed only in a Nb film and there only from edges strongly inclined relative to the main axis of the antidot lattice⁹.

Figure 2 shows the results of three different experiments, all of them carried out at $T = 3$ K with $H = 1.4$ Oe. The images are colored red, green and blue, so that overlapping penetrations in all three experiments appear as shades of gray, whereas non-repetitive flux patterns combine in color. Evidently, there is essentially no overlap in the dendritic flux patterns formed in the three experiments. The background flux penetration, however, is fully reproducible.

The origin of dendritic avalanches in superconducting films is a thermomagnetic instability mechanism between the Joule heating created by vortex motion and the reduction of the critical current density as temperature increases. The instability is also a consequence of the non-linear material characteristics of type II superconductors, which is conventionally approximated by a power law

$$\mathbf{E} = \frac{\rho_0}{d} \left(\frac{J}{J_c} \right)^{n-1} \mathbf{J}, \quad (1)$$

where \mathbf{E} is electric field, \mathbf{J} is sheet current, $J = |\mathbf{J}|$, ρ_0 is a resistivity constant, d is sample thickness, J_c is critical sheet current, and n is the creep exponent. The temperature dependencies are taken as

$$J_c = J_{c0}(1 - T/T_c), \quad n = n_1/T, \quad (2)$$

where T_c is the critical temperature. The electrodynamic

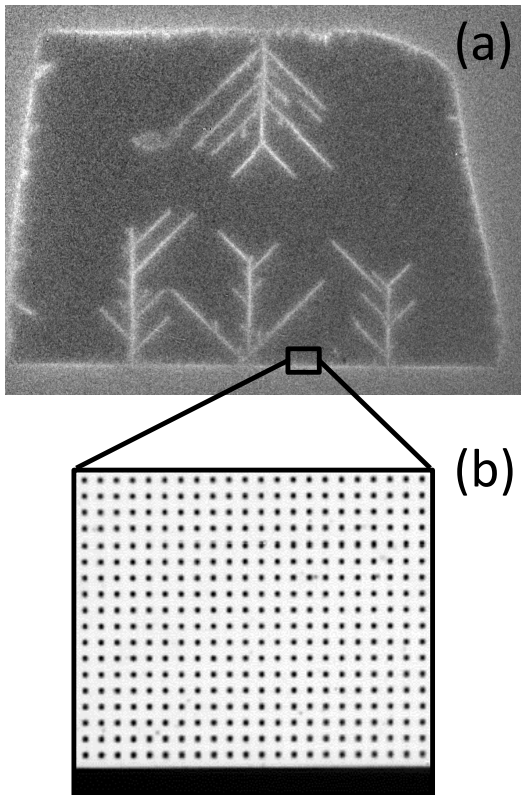


FIG. 1: (a) Magneto optical image of flux penetration at $T = 4.5$ K and $H = 1$ Oe, applied perpendicular to the film. The image brightness represents the magnitude of the local flux density. (b) Optical image of the square lattice of square antidots.

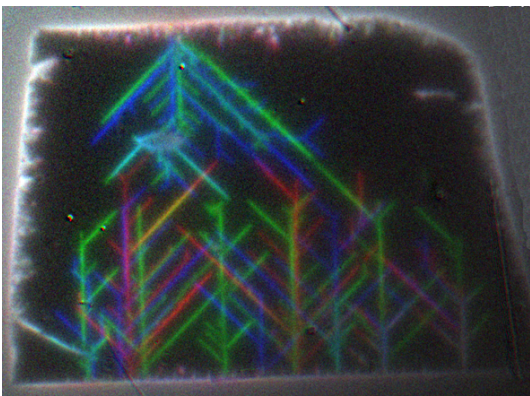


FIG. 2: Overlay of 3 repeated identical MOI experiments showing the flux penetration into the a -MoGe film, carried out at $T = 3$ K with $H = 1.4$ Oe. Each experiment is color coded in red, green and blue, thus the presence of these colors in the overlay shows that the penetration is non-reproducible.

ics must be supplemented by the heat diffusion equation

$$c\dot{T} = \kappa\nabla^2 T - \frac{h}{d}(T - T_0) + \frac{1}{d}JE, \quad (3)$$

where c is specific heat, κ is thermal conductivity, h is the coefficient for heat removal to the substrate, and T_0 is the substrate temperature.

Eq. (3) must be solved together with Maxwell's equations and the material law, Eq. (1). The description of the simulation method is found in Ref. 14, so here only the key ingredients are outlined. The main challenge is to invert the Biot-Savart law in an efficient way. This is done by including also the vacuum outside the sample in the simulation formalism. At the cost of including the extra space, one can use a real space/Fourier space hybrid method with the very attractive performance scaling of $O(N \log N)$, where N is the number of grid points.

The area of the sample was discretized on a 512×512 grid, with the geometry of strip, emulated by periodic boundary conditions. A total number of 43×43 square antidots were imposed, so that the antidot coverage was $1/4$ of the total area. The initial state of the simulation was prepared by ramping the external field with thermal feedback turned off, so that a critical state was formed from the edges. When later, the thermal feedback was turned on, and at the same time a local spot close to the edge was heated above T_c , a flux avalanche developed from the heated spot.

Figure 3 shows a map of the local flux density obtained by the numerical simulation. The avalanche of the figure demonstrates a pronounced guidance effect, contrary to the case of plain films or films patterned with random disorder. Just as in the experiments, there is a main



FIG. 3: Results of numerical calculations of the flux penetration into a superconducting film with a square array of square antidots where a thermomagnetic feedback is taken into account. Details of the numerical procedure will be published elsewhere.

trunk perpendicular to the edge and two main branches forming an angle of 45 degrees with both the edge and the directions of the antidot lattice.

In summary, we have employed MOI to observe flux avalanches in superconducting films of α -MoGe decorated with a square lattice of square antidots. Avalanches have the form of trees where the main trunk is perpendicular to the sample edge, whereas its branches form an angle of 45 degrees with the main axes of the antidot lattice. The overall features of the avalanches, and in particular the 45 degree direction of the branches, were confirmed

by numerical simulations.

This work was partially supported by the Methusalem Funding of the Flemish Government, the NES-ESF program, the Belgian IAP, the Fund for Scientific Research-Flanders (FWO-Vlaanderen), the UK Engineering and Physical Sciences Research Council and by the Brazilian funding agencies FAPESP and CNPq. AVS is grateful for the support from the FWO-Vlaanderen. THJ acknowledges the financial support of the Norwegian Research Council.

¹ C. A. Duran et al., Phys. Rev. B **52**, 75 (1995).

² T.H. Johansen, M. Baziljevich, D.V. Shantsev, P.E. Goa, Y.M. Galperin, W.N. Kang, H.J. Kim, E.M. Choi, M.-S. Kim, S.I. Lee, Supercond. Sci. Tech. **14** (2001) 726-728.

³ T.H. Johansen, M. Baziljevich, D.V. Shantsev, P.E. Goa, Y.M. Galperin, W.N. Kang, H.J. Kim, E.M. Choi, M.-S. Kim, S. I. Lee, Europhys. Lett. **59**, 599 (2002).

⁴ I.A. Rudnev, S.V. Antonenko, D.V. Shantsev, T.H. Johansen, A.E. Primenko, Cryogenics **43**, 663 (2003).

⁵ I.A. Rudnev, D.V. Shantsev, T.H. Johansen, A.E. Primenko, Appl. Phys. Lett. **87**, 042502 (2005).

⁶ S. C. Wimbush, B. Holzapfel, and C. Jooss, J. Appl. Phys. **96**, 3589 (2004).

⁷ P. Leiderer et al., Phys. Rev. Lett. **71**, 2646 (1993).

⁸ S. Hebert, L. Van Look, L. Weckhuysen, V. V. Moshchalkov, Phys. Rev. B **67** (2003) 224510.

⁹ V. Vlasko-Vlasov, U. Welp, V. Metlushko, and G. W. Crabtree, Physica C **341-348** (2000) 1281.

¹⁰ M. Menghini, R. J. Wijngaarden, A. V. Silhanek, S. Raedts, and V. V. Moshchalkov, Phys. Rev. B **71**, 104506 (2005).

¹¹ Matching effects are less pronounced at the temperature interval reported here (i.e., not very close to T_c). The commensurability field, characteristic of the lattice of ADs, is a reference for the window of magnetic fields at which the events treated here take place.

¹² V.V. Schmidt, The Physics of Superconductors, edited by P. Muller and A. V. Ustinov (Springer, Berlin-Heidelberg (1997).

¹³ L. E. Helseth et al., Phys. Rev. B **64**, 174406 (2001)

¹⁴ J. I. Vestgarden et al., Phys. Rev. B **84**, 054537 (2011)